Cancer Research

Deubiquitinase Inhibition by Small-Molecule WP1130 Triggers Aggresome Formation and Tumor Cell Apoptosis

Vaibhav Kapuria[1,2], Luke F. Peterson[1], Dexing Fang[1], William G. Bornmann[3], Moshe Talpaz[1], and Nicholas J. Donato[1]

Abstract

Recent evidence suggests that several deubiquitinases (DUB) are overexpressed or activated in tumor cells and many contribute to the transformed phenotype. Agents with DUB inhibitory activity may therefore have therapeutic value. In this study, we describe the mechanism of action of WP1130, a small molecule derived from a compound with Janus-activated kinase 2 (JAK2) kinase inhibitory activity. WP1130 induces rapid accumulation of polyubiquitinated (K48/K63-linked) proteins into juxtanuclear aggresomes, without affecting 20S proteasome activity. WP1130 acts as a partly selective DUB inhibitor, directly inhibiting DUB activity of USP9x, USP5, USP14, and UCH37, which are known to regulate survival protein stability and 26S proteasome function. WP1130-mediated inhibition of tumor-activated DUBs results in downregulation of antiapoptotic and upregulation of proapoptotic proteins, such as MCL-1 and p53. Our results show that chemical modification of a previously described JAK2 inhibitor results in the unexpected discovery of a novel DUB inhibitor with a unique antitumor mechanism. *Cancer Res; 70(22); 9265–76. ©2010 AACR.*

Introduction

Ubiquitination is a covalent posttranslational modification of cellular proteins involving a complex enzymatic cascade. Emerging evidence suggests that many enzymes of the ubiquitination cascade are differentially expressed or activated in several diseases, including cancer, and may therefore be appropriate therapeutic targets. Small molecules that affect protein ubiquitination and induce tumor cell apoptosis through inhibition of the ubiquitin conjugation or deconjugation enzymes have been described. Novel compounds that affect E1-activating enzyme activity (1–3) or E3 ligase substrate recognition such as HDM2 and TRAF6 (4, 5) have been described, and preclinical antitumor activity has been reported. Other compounds that affect protein ubiquitination indirectly have also been described, some with important clinical effect. Bortezomib is one example of such compound that specifically inhibits the chymotryptic-like activity of the 20S proteasome, resulting in the accumulation of ubiquitinated proteins. Bortezomib has been approved by the U.S. Food and Drug Administration for treatment of multiple myeloma (6) and mantle cell lymphoma (7).

Protein ubiquitination is a dynamic two-way process that can be reversed or regulated by deubiquitinating enzymes (DUB). The human genome codes for ~100 proteins with putative DUB activity (8), which can be broadly divided into two subgroups: ubiquitin COOH-terminal hydrolase (UCH) and the ubiquitin-specific proteases (USP; ref. 9). USPs comprise the largest subclass of DUBs in humans, whereas only four known UCH DUBs have been described (8). DUBs primarily serve to counterbalance ubiquitin-protein conjugation and also facilitate the cleavage of ubiquitin from its precursors and unanchored polyubiquitin chains (9). Thus, DUBs regulate and maintain the homeostasis of free ubiquitin pools in the cell (10). Several DUBs have been reported to regulate deubiquitination of histones (11), DNA damage repair (12), cellular proliferation (USP2; ref. 13), and cytokine signaling (DUB-A; ref. 14). DUBs such as USP14, UCH37, and RPN11 have been shown to associate with the regulatory subunit of proteasome (19S) and edit polyubiquitin chains on proteasome substrates (15).

Owing to the diverse role of DUBs in the regulation of proteins involved in transformation, cell cycle regulation, apoptotic protection, and drug resistance (reviewed in refs. 10, 16), DUBs seem to represent appropriate therapeutic targets. Recently, downregulation of USP2 and USP9x was shown to inhibit tumor cell growth by promoting cyclin D1 and MCL-1 degradation, respectively (13, 17), suggesting that silencing of specific DUBs in tumor cells may be a safe and effective therapy in oncogene-addicted or drug-resistant cells. Other studies firmly establish a role for DUBs in a broad spectrum of diseases including cancer (18), viral and bacterial

Authors' Affiliations: [1]Division of Hematology-Oncology, Department of Internal Medicine, University of Michigan Comprehensive Cancer Center, Ann Arbor, Michigan and [2]Graduate School of Biomedical Sciences, University of Texas Health Science Center; [3]Department of Experimental Therapeutics, M.D. Anderson Cancer Center, Houston, Texas

Note: Supplementary data for this article are available at Cancer Research Online (http://cancerres.aacrjournals.org/).

Corresponding Author: Nicholas J. Donato, Division of Hematology-Oncology, Department of Internal Medicine, University of Michigan Comprehensive Cancer Center, 1500 East Medical Center Drive, Ann Arbor, MI 48109. Phone: 734-615-5542; Fax: 734-647-9654; E-mail: ndonato@med.umich.edu.

doi: 10.1158/0008-5472.CAN-10-1530

pathogenesis (19, 20), as well as neurodegenerative disorders (21, 22). Although few compounds have been described with DUB modulatory activity, most report antitumor, antiproliferative, or antiviral activity associated with DUB inhibition [UCH-L1 (23, 24), USP7 (25), and SARS protease (19)].

WP1130 is a small molecule that was initially identified in cell-based screens for Janus-activated kinase (JAK)–signal transducer and activator of transcription (STAT) pathway inhibitors. A synthetic library of tyrphostin AG490 structural analogues was subjected to extensive structure-activity relationship (SAR) analysis coupled with chemical synthesis of compounds with increasing activity as STAT activation inhibitors. The antiproliferative and apoptotic effects of WP1130 and less active derivatives (WP1066 and WP1034) against various tumors have recently been reported in chronic myelogenous leukemia (CML; ref. 26), melanoma (27), glioblastoma (28), and myeloproliferative disorders (29). However, unlike AG490, WP1130 did not directly inhibit JAK2 kinase activity, and the mechanism of action of WP1130 remained unclear. Here, we report that WP1130 acts as a cell-permeable DUB inhibitor, inducing a rapid and marked accumulation of protein-ubiquitin conjugates, resulting in the formation of aggresomes and tumor cell apoptosis. These activities were distinct when compared with other compounds that affect protein ubiquitination such as bortezomib. DUB inhibition was not observed with AG490 incubation, suggesting that the chemical modifications that distinguish WP1130 from its parent compound result in sharply divergent mechanisms and targets of action.

Materials and Methods

Cell culture, chemical reagents, and enzymes

Human multiple myeloma MM1.S and mantle cell lymphoma Z138 cells were grown in RPMI 1640 supplemented with 10% fetal bovine serum (FBS; Invitrogen). Adherent cell lines such as human embryonic kidney 293T (HEK293T) cells were cultivated in DMEM containing 10% FBS. All cells were cultured and maintained at 37°C in a humidified atmosphere. RPMI 1640 and DMEM were purchased from HyClone (Thermo Fisher Scientific).

WP1130 was provided by Dr. William Bornmann (University of Texas, M.D. Anderson Cancer Center, Houston, TX). Other reagents used in this study were obtained from the following sources: bortezomib (Millennium Pharmaceuticals); Mini Complete and PhosSTOP inhibitory cocktails (Roche Applied Science); MG-132, NEM (*N*-ethylmaleimide), Ub-AMC, hemagglutinin-tagged ubiquitin vinyl methyl sulfone (HA-UbVS), Suc-LLVY-AMC, 20S human proteasome, UCH-L1, UCH-L3, and USP5 (BostonBiochem); and cathepsin B substrate ZRR-AMC (Santa Cruz Biotechnology).

Plasmid and small interfering RNA transfection

Plasmids for HA-tagged ubiquitin (WT/48O/63O) were kindly provided by Dr. Bryant Darnay (University of Texas, M.D. Anderson Cancer Center). HEK293T cells (10^5 per well) were seeded into six-well plates 24 hours before transfection. HA-tagged ubiquitin (500 ng; WT/63O/48O) was used to transfect per well using Fugene HD (Roche) following the manufacturer's protocol. After overnight incubation following transfection, the cells were split into two wells and incubated for an additional 24 hours before being treated with vehicle alone (DMSO) or WP1130.

ON-TARGETplus small interfering RNA (siRNA; Thermo Fisher Scientific–Dharmacon) for USP9x and USP5 (30 nmol/L each) was used to knock down USP9x and USP5 in HEK293T cells using Lipofectamine 2000. Protein levels were estimated after 72 hours of transfection by Western blotting.

Western blotting and immunoprecipitation

Whole-cell lysates were prepared by boiling and sonicating the cell pellets in 1× Laemmli reducing sample buffer. To prepare detergent-soluble and detergent-insoluble fractions, cells were lysed in cold isotonic lysis buffer [10 mmol/L Tris-HCl (pH 7.5), 0.5% Triton X-100, 150 mmol/L NaCl along with Mini Complete and PhosSTOP] for 15 minutes on ice and centrifuged for 10 minutes at 20,000 relative centrifugal force (RCF). The clarified supernatant was used as a source of the detergent-soluble cell fraction. The detergent-insoluble fraction was extracted by sonication of the residual pellet in equal volumes of boiling 1× Laemmli reducing sample buffer. Equal volumes of cellular lysate or equal protein amounts were electrophoresed on SDS-PAGE gels, transferred to membranes, and immunoblotted. To investigate p53 ubiquitination, Z138 cells were treated with WP1130 (5 μmol/L) for 4 hours and lysed in hypertonic lysis buffer [10 mmol/L Tris-HCl (pH 7.5), 0.5% Triton X-100, 250 mmol/L NaCl, 2 mmol/L NEM along with Mini Complete and PhosSTOP]. Cellular lysate (500 μg) was used to immunoprecipitate p53, and Western blotting was performed to examine changes in p53 ubiquitination after WP1130/AG490 treatment.

Antibodies used in this study were purchased from the following sources: anti-actin (Sigma-Aldrich); anti-ubiquitin clone P4D1, anti-HDAC6, anti-20S proteasome, anti-HDAC6, and goat anti-rabbit/mouse/rat IgG-conjugated horseradish peroxidase (Santa Cruz Biotechnology); anti–MCL-1 (BD Biosciences); anti-p53 (Millipore); anti-USP9x and anti-USP5 (Bethyl Laboratories); anti–poly(ADP-ribose) polymerase (PARP; Cell Signaling Technology); and anti-HA (clone 3F10; Roche Applied Science).

Proteasome activity assay

Fluorogenic Suc-LLVY-AMC substrate was used to assay for chymotryptic-like activity of the 20S proteasome. To assay for *in vivo* proteasome inhibition, Z138 cells were treated with WP1130 (5 μmol/L) or MG132 (5 μmol/L) for 2 hours. The cells were lysed in ice-cold lysis buffer [50 mmol/L HEPES (pH 7.5), 5 mmol/L EDTA, 150 mmol/L NaCl, and 1% Triton X-100], and their lysates were clarified by centrifugation at 20,000 RCF for 10 minutes. Equal amounts of protein from each sample were then incubated at 37°C with 100 μmol/L fluorogenic substrate. To assay for direct inhibition of the 20S proteasome *in vitro*, purified 20S human proteasome (200 ng) was incubated with WP1130 (5 μmol/L) or MG132 (5 μmol/L) for 30 minutes at 37°C before the addition of substrate. Fluorescence intensity was measured using a

spectrophotometer at excitation of 360 nm and emission of 460 nm. Assays were performed in triplicate, and statistical significance was determined with a paired Student's *t* test.

Cathepsin B activity assay

Cathepsin B activity was estimated as described by Foghsgaard and colleagues (30). Briefly, 20 μg of lysate from untreated, WP1130-treated (5 μmol/L, indicated time period), and leupeptin-treated (50 mmol/L, indicated time period) cells were used to assay cathepsin B activity by adding 50 μmol/L Z-Arg-Arg-AMC (zRR-AMC) in cathepsin B reaction buffer [50 mmol/L sodium acetate, 4 mmol/L EDTA, 8 mmol/L DTT, 1 mmol/L phenylmethylsulfonyl fluoride (pH 6.0)]. Fluorescence intensity was measured using a spectrophotometer at excitation of 360 nm and emission of 460 nm. Assays were performed in triplicate, and statistical significance was determined with a paired Student's *t* test.

Confocal microscopy

HEK293T cells growing on poly-lysine–coated chamber slides were treated with WP1130 or DMSO for 4 hours and washed twice in PBS followed by fixation using 4% formaldehyde for 15 minutes. The cells were permeabilized in 0.5% Triton X-100 for 5 minutes. Slides were then incubated in blocking solution (5% goat serum) for 1 hour at room temperature. Incubation with the primary antibodies (1:100) was carried out overnight at 4°C, and the slides were washed three times with 0.2% Triton X-100/PBS. Alexa Fluor anti-mouse and Alexa Fluor anti-rabbit immunoglobulin antibodies were used as secondary antibodies. The slides were washed three times and stained for nucleus detection with Hoechst 33342. To stain for aggregates of ubiquitinated proteins in mantle cell lymphoma cells, Z138 cells were treated with WP1130 for 8 hours, followed by washing in PBS. The cells were then cytocentrifuged (700 rpm, 5 minutes; Cytopro, Wescor) onto poly-lysine slides. A similar protocol (as described for HEK293T) was used to fix, permeabilize, and stain Z138 cells. Images were acquired using an Olympus FluoView 500. Images represent grouped Z-stacks (Z = 0.5 μm) from each sample.

Cell proliferation assessment by MTT and apoptosis analysis

Cells were seeded in a 96-well plate at 5,000 per well in the presence of the indicated concentration of WP1130 for 3 days in a CO_2 incubator at 37°C. Twenty microliters of 5 g/L MTT solution were added to each well for 2 hours at 37°C. The cells were then lysed in 10% SDS buffer, and absorbance at 570 nm relative to a reference wavelength of 630 nm was determined with a microplate reader. The concentrations resulting in 50% inhibition of cell growth (IC_{50} values) were calculated.

Annexin V and propidium iodide staining were used to measure apoptosis in WP1130-treated cells. Briefly, 10^5 cells/mL were harvested from tissue culture plates and centrifuged at 2,500 rpm for 5 minutes at room temperature. Medium supernatant was removed and cells were washed once in PBS. Cells were then resuspended in 0.4 mL of cold Annexin V binding buffer, and Annexin V–FITC and propidium iodide were added. Samples were incubated at room temperature for 10 minutes in the dark, filtered through nylon mesh, and analyzed by flow cytometry using a FACScan analyzer (Becton Dickinson).

In vitro deubiquitination assays

Ub-AMC protease assay. Cells were lysed in ice-cold DUB buffer containing 50 mmol/L Tris-HCl (pH 7.5), 250 mmol/L sucrose, 5 mmol/L $MgCl_2$, and 1 mmol/L phenylmethylsulfonyl fluoride by mild sonication. Briefly, 5 μg of clarified lysate from untreated, WP1130-treated, and bortezomib-treated cells were incubated with 500 nmol/L Ub-AMC in a 100-μL reaction volume at 37°C, and the release of AMC fluorescence per minute was recorded at excitation/emission of 380/460 nm using a spectrofluorometer.

Purified DUBs at optimal concentrations (USP5, 50 nmol/L; UCH-L1, 20 nmol/L; UCH-L3, 5 nmol/L; USP9x, immunoprecipitated from 500 μg Z138 cell lysate) were incubated in DUB buffer containing WP1130 (indicated concentration), vehicle alone (DMSO), or 1 mmol/L NEM (positive control for DUB inhibition) in a 100-μL reaction volume for 30 to 60 minutes at 37°C. The reaction was initiated by the addition of 500 nmol/L Ub-AMC, and the release of AMC fluorescence was recorded at excitation/emission of 380/480 using a spectrofluorometer.

Ubiquitin chain disassembly. *In vitro* disassembly of purified polyubiquitin chains (K48/K63 linked) was performed as described earlier (31). Lysate (5 μg) from untreated and WP1130-treated Z138 cells prepared in DUB buffer was incubated with K48- or K63-linked chains (1 μg) for 5, 10, and 15 minutes at 37°C. The extent of chain disassembly was assessed by Western blotting.

DUB labeling assays

To assay for changes in activity of cellular DUB enzymes, Z138 and HEK293T cells were lysed in DUB buffer for 10 minutes at 4°C. The lysates were centrifuged at 20,000 RFC for 10 minutes, and the supernatant was used for DUB labeling as previously described (32, 33). Equal amounts of lysate were incubated with 500 ng of HA-UbVS for 1 hour at room temperature, followed by boiling in reducing sample buffer and resolving by SDS-PAGE. After protein transfer to nitrocellulose membranes, HA immunoblotting was used to detect DUB labeling.

Results

Our preliminary studies showed that mantle cell lymphoma Z138 cells displayed high apoptotic sensitivity to WP1130 (IC_{50} ~1 μmol/L), evident by the appearance of cleaved PARP after 2 to 4 hours of treatment. Direct comparison of WP1130 with AG490 or bortezomib, which is clinically active in mantle cell tumors, illustrated distinctions in the apoptotic onset and activity of each compound (Fig. 1A). WP1130 displayed potent antiproliferative properties against various other tumor cell lines of myeloid and lymphoid origin as well as HEK293T cells (Supplementary Fig. S1A and B). Because WP1130 showed no direct inhibition of JAK2 kinase activity, we investigated other cellular activities that may underlie the apoptotic activity of WP1130. Molecular analysis revealed some structural and chemical similarities between WP1130

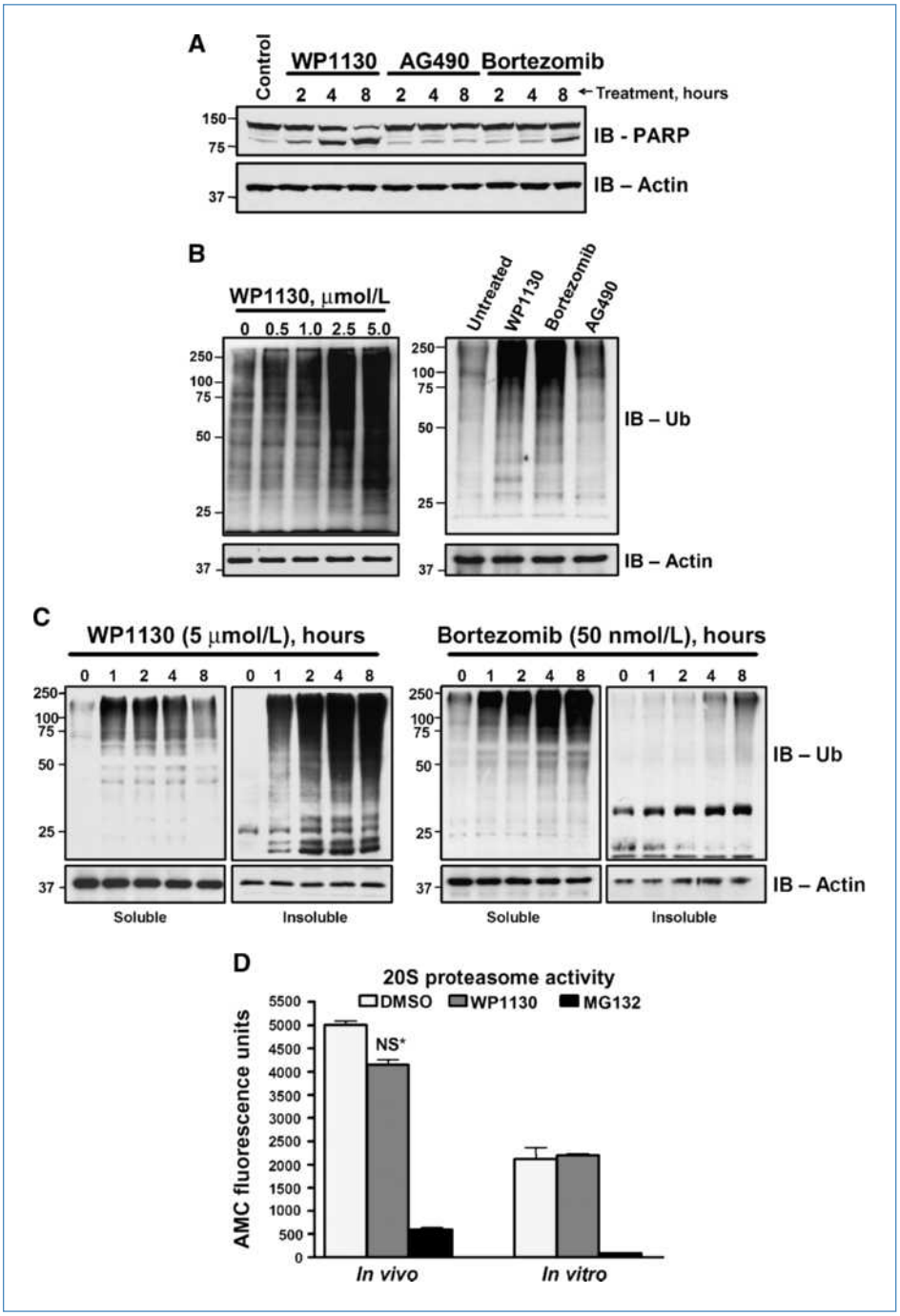

Figure 1. WP1130 induces accumulation of ubiquitinated proteins without proteasome inhibition. A, mantle cell lymphoma (Z138) cells were treated with WP1130 (5 μmol/L), AG490 (100 μmol/L), or bortezomib (50 nmol/L) for the interval indicated. Whole-cell extracts were probed for detection of cleaved PARP as an indicator for the onset of apoptosis. Actin was probed on the same blot as a protein loading control. B, left, Z138 cells were incubated with the indicated concentration of WP1130 for 2 h before whole-cell lysates were subjected to immunoblotting with anti-ubiquitin; right, Z138 cells were treated with 5 μmol/L WP1130, 50 nmol/L bortezomib, or 100 μmol/L AG490 for 2 h before their extracts were probed for the presence of ubiquitinated proteins. Membranes were probed for actin as a protein loading control. C, Z138 cells were treated with either WP1130 or bortezomib for the interval indicated. Lysates were separated into detergent-soluble and detergent-insoluble fractions as described in Materials and Methods and probed for the distribution of ubiquitinated proteins and actin (as a protein loading control) by immunoblotting. D, left (*In vivo*), lysates from control (DMSO), WP1130-treated, or MG-132–treated cells (5 μmol/L, 2 h) were analyzed for proteasome activity as described in Materials and Methods; right (*In vitro*), purified 20S proteasome was incubated with 5 μmol/L WP1130, 5 μmol/L MG-132, or vehicle alone (DMSO) for 30 min before analysis of proteasome activity by monitoring substrate cleavage. Columns, average of triplicate samples; bars, SD.

and a few compounds with described DUB inhibitory activity, such as dibenzylideneacetone (DBA) and curcumin (34). These observations prompted a detailed analysis of the effects of WP1130 on cellular protein ubiquitination.

WP1130 induces rapid ubiquitination without affecting proteasome activity

Analysis of whole-cell extracts from WP1130-treated Z138 cells showed a marked and concentration-dependent accumulation of ubiquitinated proteins (Fig. 1B, left). A similar increase in protein ubiquitination was seen in other WP1130-treated cells, including K562, MM.1S, BV173, HeLa, and HEK293T (data not shown). In contrast to WP1130 and the proteasome inhibitor bortezomib, AG490 treatment did not induce a change in cellular protein ubiquitination in Z138 cells (Fig. 1B, right), even after longer incubation intervals (data not shown), suggesting distinct mechanisms of action for WP1130 and its parent AG490 compound.

We further observed a rapid, time-dependent accumulation of ubiquitinated proteins into both the detergent-soluble and detergent-insoluble fraction of WP1130-treated Z138 cells (Fig. 1C). These results suggested distinct mechanisms and downstream effectors of protein ubiquitination in WP1130- and bortezomib-treated cells. Because the accumulation of ubiquitinated proteins occurs following proteasome inhibition, we assessed the effect of WP1130 on 20S proteasome activity. As shown in Fig. 1D, WP1130 incubation (5 μmol/L, 2 hours) caused no significant decline in proteasome chymotryptic-like activity *in vivo* ($P > 0.07$) and *in vitro* ($P > 0.78$), whereas the proteasome inhibitor MG-132 substantially inhibited proteasome activity in either assay. These results suggest that unlike MG-132 or bortezomib, WP1130 does not directly block 20S proteasomal activity. Oxidative stress has also been implicated in accumulation of ubiquitinated proteins (35). However, we did not detect an increase in the generation of reactive oxygen species in WP1130-treated cells (Supplementary Fig. S2A).

To further define the ubiquitin linkages accumulating in response to WP1130, we transfected HEK293T cells with plasmids expressing HA-tagged variants of ubiquitin (WT/K48Only/K63Only). Treatment of HEK293T transfectants with WP1130 showed increased accumulation of ubiquitinated proteins containing both K48- and K63-linked polyubiquitin chains (Supplementary Fig. S2B). Proteasomal inhibition leads to the accumulation of proteins containing K48-linked ubiquitin chains while having limited effect on K63-linked ubiquitin chains (36). Therefore, these results further suggest distinctions between WP1130-mediated and proteasome inhibition–mediated ubiquitination.

Aggresome formation

Ubiquitinated insoluble aggregates of protein are commonlyassociated with perinuclear structures called aggresomes (37). Proteasome inhibition, unfolded protein response, heat shock response, or oxidative stress can lead to aggresome formation (38). Aggresomes are rich in HSP90/70, 20S proteasome, and HDAC6 content in conjunction with poly-ubiquitinated proteins (39). Because we consistently noted a rapid accumulation of ubiquitinated proteins in the detergent-insoluble fraction on WP1130 treatment, we performed confocal microscopy of WP1130-treated HEK293T cells to determine whether we could detect aggresome-like structures using key aggresome markers such as ubiquitin, HDAC6, and 20S proteasome. We observed juxtanuclear deposition of poly-ubiquitinated proteins, colocalizing with aggresome markers in WP1130-treated cells (Fig. 2A and B). Dense aggregates of ubiquitinated proteins were also observed in WP1130-treated Z138 cells (Supplementary Fig. S3A). Additionally, the HDAC6 inhibitor trichostatin A (TSA) blocked WP1130-induced aggresome formation. Cells pretreated with TSA (1 μmol/L) followed by 8 hours of incubation with WP1130 (5 μmol/L) failed to form visible, dense, perinuclear-localized aggresomes and contained smaller aggregates of ubiquitinated proteins dispersed throughout the cytoplasm (Supplementary Fig. S3A). Although proteasome inhibition has been shown to induce aggresome formation, prolonged treatment of the cells with bortezomib (~24 hours) is often required (40). We compared WP1130-mediated aggresome formation with aggresome formation following proteasome inhibition (MG-132) in Z138 cells. WP1130 treatment led to early formation (4 hours) of perinuclear-dense aggregates of ubiquitinated proteins, whereas MG-132–treated Z138 cells showed aggresome-like structures on prolonged incubation (Supplementary Fig. S3B). These results show that WP1130 can induce aggresome formation through a distinct mechanism that is independent of 20S proteasome inhibition.

WP1130 acts as DUB inhibitor

Inhibition of cellular DUBs could also lead to an increase in high–molecular weight ubiquitinated proteins in the absence of proteasome inhibition (23, 41). As described earlier, WP1130 shares some structural and chemical resemblance to known DUB inhibitors. Therefore, we assessed possible indications of DUB inhibition in WP1130-treated cells. We observed a rapid depletion of monomeric ubiquitin (Fig. 3A) and a subsequent increase in the levels of unanchored/free polyubiquitin chains ($Ub_{4\text{-}6}$) in cells treated with WP1130 (Fig. 3B). In contrast, bortezomib treatment did not significantly affect the level of free ubiquitin or unanchored ubiquitin chains. This observation suggests that WP1130 may reduce ubiquitin recycling and amass ubiquitinated proteins through inhibition of DUB activity. To directly assess the effect of WP1130 on DUB activity in treated cells, cell lysates from control and treated cells were incubated with Ub-AMC and fluorescence generated as a consequence of substrate cleavage was measured as an indicator of DUB activity. Treatment with WP1130 significantly reduced DUB activity in Z138 cells by ~50% by 4 hours ($P = 0.0095$). Interestingly, we did not see any change in DUB activity in bortezomib-treated cells, whereas NEM (known DUB inhibitor) suppressed cellular DUB activity by 80% within 1 hour (Fig. 3C).

We also examined the effect of WP1130 treatment on *in vitro* deubiquitination/disassembly of purified K48- or K63-linked polyubiquitin chains. Lysates from WP1130-treated (2 hours) or untreated cells were incubated with 1 μg of unanchored polyubiquitin chains for 5, 10, and 15 minutes at 37°C. Lysates from untreated cells displayed an almost complete disassembly of polyubiquitin chains in contrast to the limited disassembly observed with lysates from WP1130-treated cells (Fig. 3D). Lack of chain disassembly of both K48- and K63-linked polyubiquitin chains from the lysates of WP1130-treated cells agrees with our previous observations of increased accumulation of both types of ubiquitin linkages on WP1130 treatment (Supplementary Fig. S2B). These results suggest that WP1130 treatment inhibits cellular DUB enzyme/s required for the breakdown of both K48- and K63-specific ubiquitin linkages.

WP1130 inhibits DUB enzymes *in vitro*

To further assess DUB inhibition in WP1130-treated cells, we used a technique described by Borodovsky and colleagues

(32, 33) to identify the profile of active cellular DUB activity in intact cells. HA-UbVS acts as a DUB suicide substrate, forming a covalent adduct with active DUB enzymes. Specific cellular DUBs can be identified by anti-HA blotting, as previously shown in various cell types (32, 42, 43). Changes in specific DUB activities are measurable by monitoring HA labeling in lysates from control and treated cells. A dose- and time-dependent reduction in the labeling of DUBs representing USP9x, USP5, USP14, and UCH37 was seen in cells treated with WP1130 (Fig. 4A and B). In contrast, no change in DUB labeling was noted in cells treated with AG490, confirming distinctions in the activity and mechanism of action of the parental tyrphostin and WP1130. An *in vitro* analysis using cell lysates was performed to investigate direct DUB inhibition by WP1130. Briefly, untreated Z138 cell lysates were incubated with 5 μmol/L WP1130 or vehicle alone for 1 hour at 37°C, followed by labeling with HA-UbVS. Incubation of cell lysate with WP1130 showed a reduction of HA labeling of the same DUBs as those noted in intact cells (Fig. 4C), suggesting that WP1130 caused direct DUB inhibition.

To determine whether WP1130 directly inhibits DUB activity, we incubated purified DUBs such as USP5, UCH-L1, and UCH-L3 with vehicle alone or varied concentrations of WP1130 for 30 minutes in DUB buffer at 37°C. USP9x was immunoprecipitated from Z138 cell lysates and prepared in DUB buffer, and the beads were incubated with vehicle alone or WP1130 for 30 minutes. Ub-AMC (500 nmol/L) was added to each reaction, and fluorescence was monitored every minute for up to 30 minutes. The maximum fluorescence observed at the end of the linear phase of substrate cleavage in control and WP1130-treated DUB assays was used as a gauge to estimate % inhibition of DUB activity. As shown in Fig. 5A, treatment with 5 μmol/L WP1130 reduced the activities of USP9x, USP5, and UCH-L1 by ≥80% (detail in Supplementary Fig. S4). No inhibition was observed against UCH-L3 activity, suggesting that WP1130 may be partly selective. We confirmed the loss of USP5 activity using HA-UbVS labeling, which showed ~80% reduction in HA labeling on incubation with WP1130 (Fig. 5B). Because deubiquitinating enzymes are cysteine proteases, we

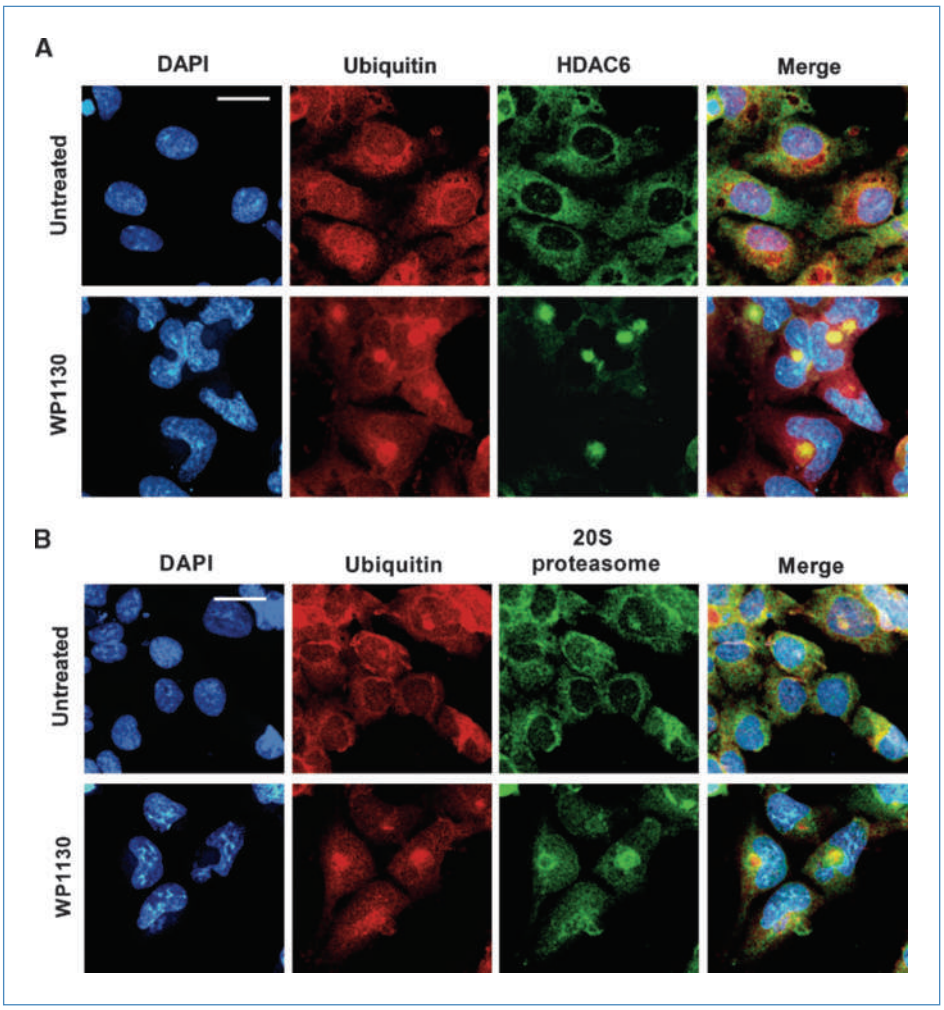

Figure 2. WP1130 treatment induces aggresome formation. A and B, control or WP1130-treated (5 μmol/L, 4 h) HEK293T cells were processed for immunofluorescence as described in Materials and Methods. Treatment with WP1130 led to perinuclear accumulation of aggresome markers such as ubiquitin (red), HDAC6 (green), and 20S proteasome (green). Images were acquired using Olympus FluoView 500 confocal microscope using 60× water immersion lens and 2× digital zoom (×120 total magnification).

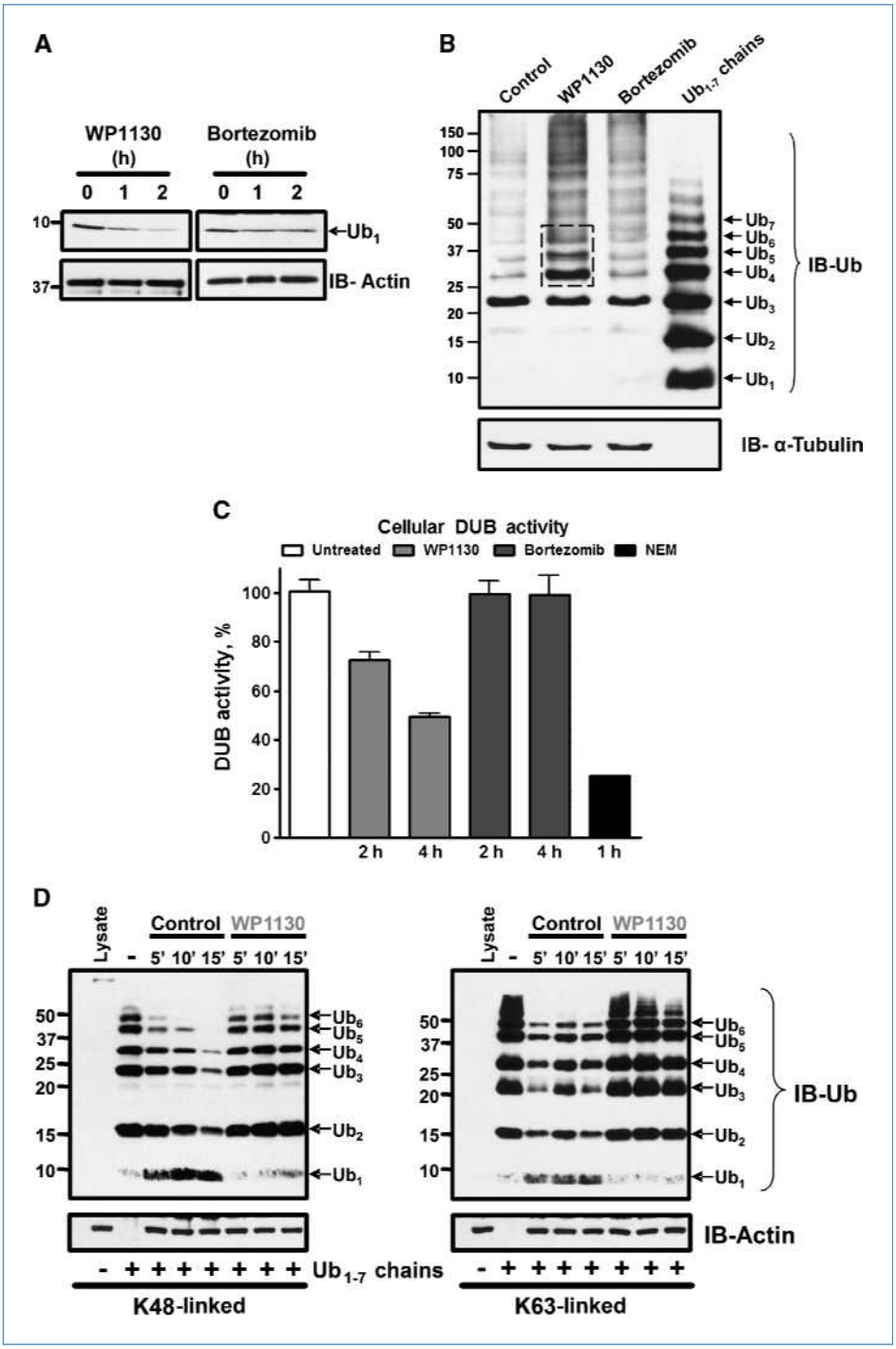

Figure 3. WP1130 reduces cellular deubiquitinating activity. A, Z138 cells were incubated with WP1130 (5 μmol/L) or bortezomib (50 nmol/L) for the indicated intervals. Whole-cell extracts were probed for the levels of monoubiquitin by running high percent (15%) gels and immunoblotting. B, Z138 cells were treated with DMSO (control), 5 μmol/L WP1130, or 50 nmol/L bortezomib for 2 h before whole-cell lysates were resolved on high percent cross-linked gels and subjected to immunoblotting for ubiquitin and actin. Preformed ubiquitin polymers (Ub_{1-7}) were loaded in the last lane as a marker for the relative migration of individual ubiquitin chains. C, Z138 cells were treated with 5 μmol/L WP1130, 50 nmol/L bortezomib, and 1 mmol/L NEM or untreated for the interval indicated before extracts (5 μg) were prepared as described in Materials and Methods and incubated with fluorogenic substrate. The results are representative of one analysis performed in triplicate. Similar results were obtained in two additional independent assays. D, lysates (5 μg) from vehicle-treated (DMSO) or WP1130-treated (5 μmol/L, 4 h) cells were incubated with 1 μg of K48-linked (left) or K63-linked (right) free chains of polyubiquitin (Ub_{1-7}) for 5, 10, and 15 min at 37°C. The extent of free chain hydrolysis in each lysate was examined by Western blotting. Actin was blotted as a protein loading control.

examined if WP1130 has any effect on the activity of lysosomal cysteine proteases (cathepsin B). Interestingly, we observed a time-dependent increase in cathepsin B activity from the lysates of WP1130-treated cells (Supplementary Fig. S5), which was distinct when compared with the effects of the cathepsin inhibitor leupeptin. The increased cathepsin activity in WP1130-treated cells is possibly due to increased autophagy in WP1130-treated cells (data not shown). Cathepsin B activity has been shown to be elevated in cells undergoing autophagy (44)

DUBs modulate proapoptotic and antiapoptotic protein levels

USP5 is known to play a major role in maintaining the levels of unanchored polyubiquitin chains (45). Loss of USP5 has been reported to stabilize p53 due to the accumulation

of free polyubiquitin chains, which compete with ubiquitinated p53 (31). During the preparation of this article, USP9x was shown to enhance tumor cell survival by deubiquitinating the antiapoptotic protein MCL-1, thereby promoting its stability (17). The authors showed a positive correlation between the increased levels of MCL-1 and USP9x in lymphomas and other tumors. siRNA-mediated knockdown of USP9x led to rapid degradation of MCL-1 and sensitization of tumor cells to apoptotic stimuli. Considering these recent reports, we investigated the downstream effects of inhibiting USP9x and USP5 in Z138 cells.

Consistent with published reports, we observed a dose-dependent increase in p53 and decline in MCL-1 protein levels on WP1130 treatment (Fig. 5C). Cotreatment of Z138 cells with cycloheximide (50 μg/mL) and WP1130 confirmed the stabilization rather than induction of p53 protein, as shown in Supplementary Fig. S6. To reconfirm the role played by USP9x and USP5 in regulating the levels of MCL-1 and p53 respectively, we performed siRNA-based knockdown of USP9x and USP5 in HEK293T cells. Loss of USP9x led to ~50% decline in MCL-1 levels, whereas loss of USP5 showed ~2-fold increase in p53 levels (Fig. 5D). Together, these results show that WP1130 inhibits selective cellular DUB activities, modulating the stability of both antiapoptotic and proapoptotic proteins.

We further examined if WP1130 induced ubiquitination of p53 and MCL-1. Treatment of Z138 cells with WP1130 (5 μmol/L, 4 hours) promoted ubiquitination of p53, as shown in Fig. 6A, whereas parental tyrphostin AG490 showed no change in basal levels of p53 ubiquitination. We further observed that WP1130-mediated depletion of MCL-1 in Z138 cells was blocked only in the presence of a proteasome inhibitor (MG-132) and not caspase inhibitor (zVAD; Fig. 6B). However, potent inhibition of WP1130-sensitive DUBs (including USP9x) was still observed in the presence of MG-132 or zVAD, suggesting that the rescue of MCL-1 from

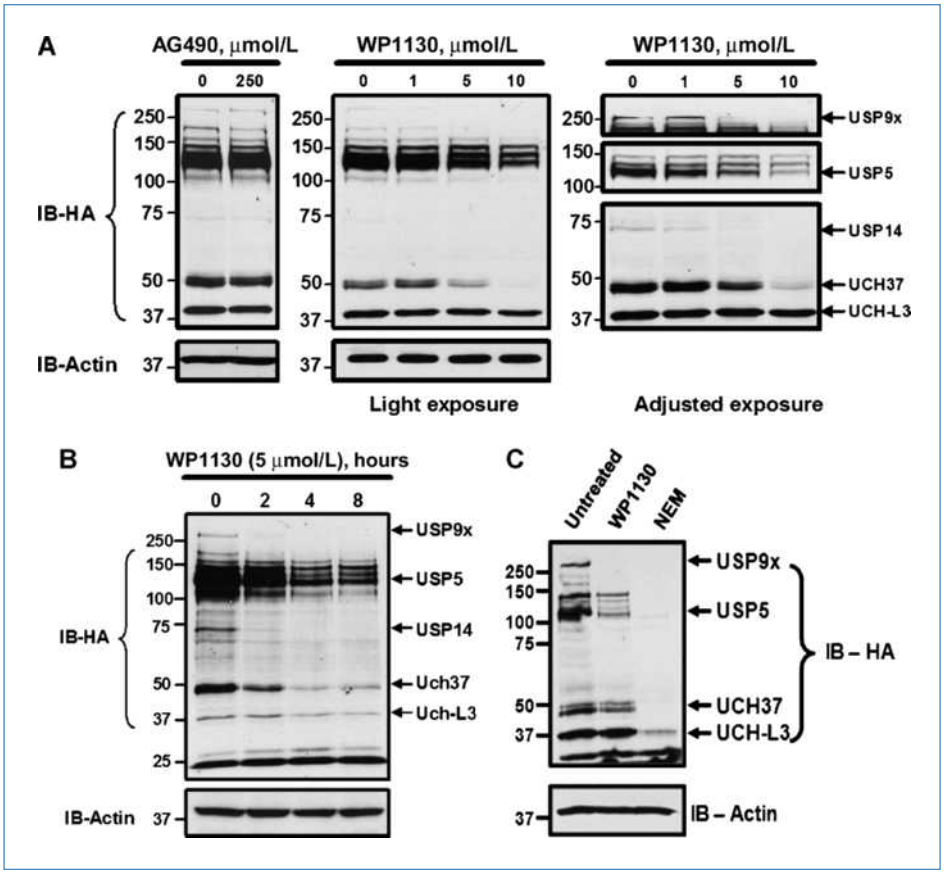

Figure 4. DUB inhibitory profile of WP1130. A, Z138 cells were treated with the indicated concentration of WP1130 or AG490 for 1 h. The cells were lysed in DUB labeling buffer as described in Materials and Methods. Clarified supernatant (20 μg) was incubated with 200 nmol/L HA-UbVS for 1 h at 37°C. HA immunoblotting was used to assess changes in DUB labeling. Actin was probed as a protein loading control. Dual exposures are shown to allow determination of DUB inhibition against DUBs with high and low labeling activity. Individual DUBs were assigned (right) based on relative electrophoretic mobility and confirmed by subsequent immunoprecipitation and immunoblotting (data not shown). B, Z138 cells were treated with 5 μmol/L WP1130 for the interval indicated followed by lysis in DUB buffer. Lysates were subjected to HA labeling and DUB assignments were made based on the criterion described in A. C, untreated Z138 cell extracts were prepared in DUB buffer as described in Materials and Methods. Lysate (20 μg) was incubated with vehicle alone (untreated/DMSO), 5 μmol/L WP1130, or 2 mmol/L NEM for 1 h at 37°C. The reaction mixture was subjected to labeling with 200 nmol/L HA-UbVS for an additional 1 h at 37°C, and DUB activity was assessed by HA immunoblotting. Actin was probed as a protein loading control.

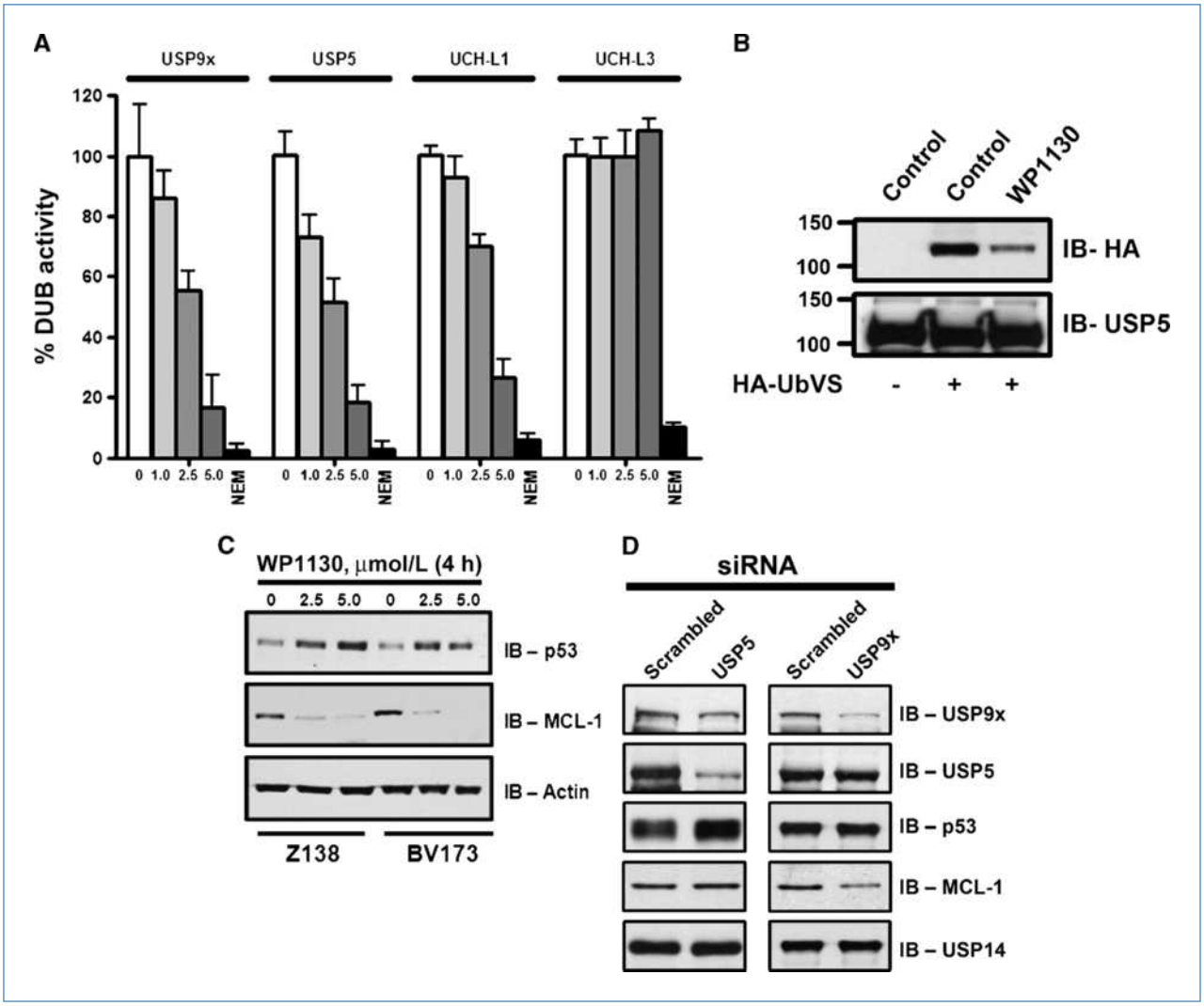

Figure 5. WP1130 inhibits purified DUBs. A, optimal concentrations of recombinant or immunopurified DUB enzyme (USP5, 50 nmol/L; UCH-L1, 50 nmol/L; UCH-L3, 5 nmol/L; USP9x, immunoisolated) were incubated in DUB activity buffer containing the indicated concentration of WP1130, 2 mmol/L NEM, or vehicle alone in a 100-μL reaction volume for 30 min at 37°C in 96-well fluorometry plates. After incubation, 500 nmol/L Ub-AMC was added to the reaction and the release of AMC fluorescence was recorded over time. The % activity for each enzyme was estimated by monitoring the change in substrate cleavage relative to controls (DMSO; representing 100% activity). Data represent the average of two independent experiments. B, recombinant USP5 (20 nmol/L) was subjected to HA-UbVS labeling in the presence of vehicle alone (DMSO) or 5 μmol/L WP1130 (30 min). Immunoblotting was used to determine USP5 activity (HA blotting; top) and protein level (USP5 blot; bottom). C, whole-cell extracts from Z138 and BV173 cells were probed for MCL-1 and p53 protein levels after 4 h of treatment with the indicated concentration of WP1130. Actin was probed as a protein loading control. D, HEK293T cells were transfected with 30 nmol/L siRNA targeting specific DUBs as described in Materials and Methods. Extent of each DUB (USP9x, USP5) knockout and their effect on previously described targets were assessed by immunoblotting for p53, MCL-1, and USP14 (negative control, no effect).

WP1130-mediated depletion in the presence of MG-132 is not due to its failure to suppress DUB activity. These results suggest that MCL-1 undergoes ubiquitination on treatment with WP1130 as a result of USP9x inhibition and is processed via proteasomal degradation.

DUB inhibition by WP1130 induces apoptosis

WP1130 contains α, β-unsaturated carbonyl group that can hypothetically interact with the sulfhydryl of cysteines found in the active sites of DUBs through a Michael addition reaction (46). However, similar carbonyl groups are found in AG490, but this molecule possesses no apparent DUB inhibitory activity in cells. Interestingly, we observed a complete loss of WP1130-induced apoptosis and its associated antiproliferative effects in the presence of DTT (Fig. 6C; Supplementary Fig. S7A). This observation correlates with the loss of induced ubiquitination (Fig. 6D) and DUB inhibition by WP1130 in the presence of DTT (Supplementary Fig. S7B and C). The loss of WP1130-induced apoptosis and DUB inhibitory activity in the presence of DTT suggests that suppression of active DUBs by WP1130 directly accounts for the apoptotic effects of WP1130.

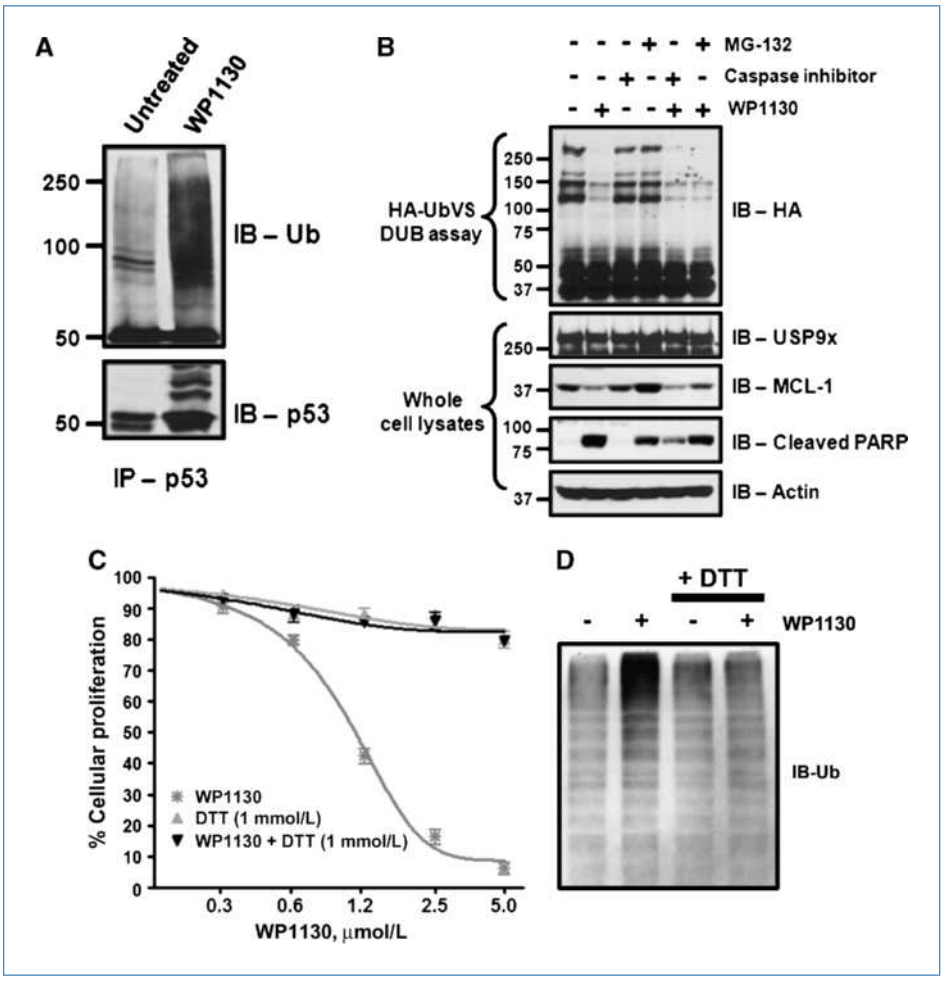

Figure 6. DUB inhibition by WP1130 induces apoptosis. A, p53 was immunoprecipitated from WP1130 (5 μmol/L)–treated or untreated Z138 cells for 4 h and immunoblotted to detect p53 ubiquitination as described in Materials and Methods. B, BV173 cells were treated with 5 μmol/L WP1130 alone or in the presence of either MG-132 (5 μmol/L) or ZVAD (20 μmol/L) for 4 h. A fraction of cells from each sample was aliquoted and processed for DUB labeling by HA-UbVS to detect DUB activity as described earlier. The remaining cells were lysed in Laemmli buffer and probed for levels of MCL-1, USP9x, cleaved PARP, and actin (loading control). C, Z138 cells were incubated with the indicated concentration of WP1130 in the presence and absence of 1 mmol/L DTT. Additionally, Z138 cells were also incubated with 1 mmol/L DTT alone as control. After 3 d of incubation, cellular proliferation was analyzed by MTT as described in Materials and Methods. D, Z138 cells were treated with 5 μmol/L WP1130 or vehicle alone (DMSO) in the presence and absence of 1 mmol/L DTT for 2 h. The levels of ubiquitinated protein were assessed by immunoblotting with anti-ubiquitin.

WP1051 and WP1052 represent two earlier chemical analogues of WP1130. During our earlier SAR investigation of cellular proliferation (by MTT) by the WP series of compounds, we noted that whereas WP1051 was effective in suppressing tumor cell proliferation (although at high doses than WP1130), WP1052 failed to show any antitumor properties (Supplementary Fig. S8A). This was unexpected as WP1051 and WP1052 are chemically identical but structurally distinct isomers. Because we had noted that the apoptosis/antiproliferative properties of WP1130 are related to its ability to suppress cellular DUBs and induce accumulation of ubiquitinated proteins, we next investigated whether WP1051 and WP1052 can affect protein ubiquitination and DUB activity. Treatment of Z138 cells with the indicated concentrations of WP1051 and WP1052 showed that whereas WP1051 can induce accumulation of ubiquitinated proteins in a dose-dependent fashion, WP1052 failed to show any effect on ubiquitinated proteins (Supplementary Fig. S8A, top). We further examined the DUB labeling profile in lysates from cells treated with WP1051 or WP1052 and observed that whereas WP1051 could suppress the activity of a DUB corresponding to USP9x, WP1052 showed no DUB inhibition. These results show that DUB inhibition by this class of compounds exhibits a precise chemical SAR.

Discussion

Ubiquitination and ubiquitin-like protein modification play a major role in directing the fate and function of most cellular proteins (47). Several key enzymes in these pathways are amplified or modified in diseased cells and provide rationale for development of small molecules that inhibit or modulate their activity. Major advances have been made in selective targeting of specific enzymes in these pathways, some with clinical effect (5). Due to the specialized role of DUBs in the ubiquitin cycle and their emerging role in control of multiple signaling pathways and oncoproteins, DUB inhibitors may be useful anticancer agents (48). In this study, we describe the unexpected DUB inhibitory activity of WP1130, a novel small molecule derived from the JAK2 inhibitor AG490. WP1130 induces accumulation of polyubiquitinated proteins and promotes tumor cell apoptosis.

Peptide-based potent, irreversible inhibitors of DUBs, such as ubiquitin aldehyde and UbVS, have been previously

described (33, 49). However, their therapeutic potential is limited by their high–molecular weight and limited cellular bioavailability. Other small-molecule compounds, such as D12-prostaglandin J2, were initially shown to inhibit ubiquitin isopeptidase activity in cells (IC_{50} ~30 μmol/L) and cause cellular accumulation of ubiquitinated proteins and cell death (41). A key molecular determinant required for DUB inhibitory activity, α, β-unsaturated ketone with sterically accessible β-carbon, was noted in this compound and led to the identification of additional inhibitors with similar activities, such as DBA (IC_{50} ~20–40 μmol/L), curcumin (IC_{50} ~80–100 μmol/L), and shikoccin (NSC-302979; IC_{50} ~15 μmol/L). However, the profile of specific DUBs affected by these compounds has not been described (34).

Using multiple *in vivo* and *in vitro* assays, we provide mechanistic evidence that WP1130 acts as a partially selective DUB inhibitor. Our data show that WP1130 suppresses the activities of major cellular DUBs such as USP5, UCH-L1, USP9x, USP14, and UCH37. Inhibition of multiple DUBs is likely to induce multiple predictable cellular changes, such as (*a*) increased accumulation of polyubiquitinated proteins/unanchored polyubiquitin chains (Figs. 1B and 3B), (*b*) decline in the pool of monomeric ubiquitin (Fig. 3A), (*c*) slower rate of polyubiquitin disassembly (Fig. 3D), (*d*) an overall decrease in individual DUB activities (Fig. 5A), and (*e*) affect cellular levels/activities of DUB-regulated oncoproteins (Fig. 5C). USP5 and UCH37 are known to deubiquitinate both K48- and K63-linked polyubiquitinated proteins (50, 51). The accumulation of K63-linked polyubiquitinated proteins in WP1130-treated HEK293T cells may partially be explained based on these findings, although there are other DUBs, such as CYLD (51), which can break such chains as well.

A marked increase in cellular ubiquitinated proteins, arising due to either proteasome inhibition or loss of cellular DUB activity, can trigger aggresome formation (23, 38). Formation of aggresomes under conditions of stress results in a temporary cellular cytoprotective event, relocating vast amounts of accumulated ubiquitinated proteins to the aggresomal insoluble fraction (40). Our recent data suggest that WP1130 treatment causes accumulation of polyubiquitinated JAK2 and Bcr-Abl into detergent-insoluble aggresomes, thereby suppressing tumor cell proliferation.[4,5] Therefore, trafficking of oncoproteins, which play a crucial role in proliferation, survival, and growth factor signaling into the aggresome, where they are unable to function, is predicted to be detrimental to tumor cells. However, the DUB(s) that plays a crucial role in regulating these oncogenic kinases is not currently known. Using xenograft mouse models of CML and melanoma, we have previously shown that WP1130 treatment effectively suppresses tumor growth *in vivo* (26). Together, these observations suggest that WP1130 may act as a therapeutic agent through its effects on DUB activity.

It is noteworthy that several of the DUBs targeted by WP1130 have recently been shown to be key regulators of the stability and turnover of specific oncogenes and apoptotic regulators, including MCL-1 (USP9x; ref. 17) and p53 (USP5; ref. 31). Other DUBs are suggested to play a direct role in transformation (18) and control of ubiquitinated protein entry into the proteasome (52). Still, others that may be targeted by WP1130 have recently been shown to play a role in unregulated cell growth and tumor cell addiction (13). The role played by many other DUBs and their effect on their cognate substrates in the apoptotic activity engaged by WP1130 is not yet known.

How WP1130 inhibits the activity of DUBs is not yet completely known. It might be possible for WP1130 to interact with the active site cysteine of DUBs, owing to the presence of an α, β-unsaturated carbonyl group in WP1130. Because such functional groups are highly susceptible to nucleophilic attack from sulfhydryl groups, this may explain the loss of DUB inhibition by WP1130 in the presence of DTT. Additionally, the full profile of DUBs that are affected by WP1130 is being further assessed. Crystal structures of several deubiquitinating enzymes have revealed a high degree of homology within their catalytic core (53, 54). This may account for the partial selectivity of WP1130 against a specific subset of DUBs. Further SAR studies to develop structural variants of WP1130 with increased target specificity may enhance antitumor-directed activities.

Disclosure of Potential Conflicts of Interest

No potential conflicts of interest were disclosed.

Grant Support

UM start up funds and UM Cancer Center Epstein and Padnos funds.

The costs of publication of this article were defrayed in part by the payment of page charges. This article must therefore be hereby marked *advertisement* in accordance with 18 U.S.C. Section 1734 solely to indicate this fact.

Received 04/28/2010; revised 08/19/2010; accepted 09/28/2010; published OnlineFirst 11/02/2010.

[4] Kapuria and colleagues, unpublished data.
[5] Sun and colleagues, unpublished data.

References

1. Kitagaki J, Yang Y, Saavedra JE, Colburn NH, Keefer LK, Perantoni AO. Nitric oxide prodrug JS-K inhibits ubiquitin E1 and kills tumor cells retaining wild-type p53. Oncogene 2009;28:619–24.
2. Yang Y, Kitagaki J, Dai RM, et al. Inhibitors of ubiquitin-activating enzyme (E1), a new class of potential cancer therapeutics. Cancer Res 2007;67:9472–81.
3. Xu GW, Ali M, Wood TE, et al. The ubiquitin-activating enzyme E1 as a therapeutic target for the treatment of leukemia and multiple myeloma. Blood 2010;115:2251–9.
4. Yang Y, Ludwig RL, Jensen JP, et al. Small molecule inhibitors of HDM2 ubiquitin ligase activity stabilize and activate p53 in cells. Cancer Cell 2005;7:547–59.
5. Guedat P, Colland F. Patented small molecule inhibitors in the ubiquitin proteasome system. BMC Biochem 2007;8 Suppl 1:S14.
6. Hideshima T, Richardson P, Chauhan D, et al. The proteasome

inhibitor PS-341 inhibits growth, induces apoptosis, and overcomes drug resistance in human multiple myeloma cells. Cancer Res 2001; 61:3071–6.
7. Goy A, Younes A, McLaughlin P, et al. Phase II study of proteasome inhibitor bortezomib in relapsed or refractory B-cell non-Hodgkin's lymphoma. J Clin Oncol 2005;23:667–75.
8. Nijman S, Luna-Vargas M, Velds A, et al. A genomic and functional inventory of deubiquitinating enzymes. Cell 2005;123:773–86.
9. Wilkinson KD. Regulation of ubiquitin-dependent processes by deubiquitinating enzymes. FASEB J 1997;11:1245–56.
10. Reyes-Turcu FE, Ventii KH, Wilkinson KD. Regulation and cellular roles of ubiquitin-specific deubiquitinating enzymes. Annu Rev Biochem 2009;78:363–97.
11. Zhang Y. Transcriptional regulation by histone ubiquitination and deubiquitination. Genes Dev 2003;17:2733–40.
12. Zhang D, Zaugg K, Mak TW, Elledge SJ. A role for the deubiquitinating enzyme USP28 in control of the DNA-damage response. Cell 2006;126:529–42.
13. Shan J, Zhao W, Gu W. Suppression of cancer cell growth by promoting cyclin D1 degradation. Mol Cell 2009;36:469–76.
14. Kayagaki N, Phung Q, Chan S, et al. DUBA: a deubiquitinase that regulates type I interferon production. Science 2007;318:1628–32.
15. Ventii KH, Wilkinson KD. Protein partners of deubiquitinating enzymes. Biochem J 2008;414:161–75.
16. Song L, Rape M. Reverse the curse—the role of deubiquitination in cell cycle control. Curr Opin Cell Biol 2008;20:156–63.
17. Schwickart M, Huang X, Lill JR, et al. Deubiquitinase USP9X stabilizes MCL1 and promotes tumour cell survival. Nature 2010; 463:103–7.
18. Hussain S, Zhang Y, Galardy PJ. DUBs and cancer: the role of deubiquitinating enzymes as oncogenes, non-oncogenes and tumor suppressors. Cell Cycle 2009;8:1688–97.
19. Ratia K, Pegan S, Takayama J, et al. A noncovalent class of papain-like protease/deubiquitinase inhibitors blocks SARS virus replication. Proc Natl Acad Sci U S A 2008;105:16119–24.
20. Rytkonen A, Poh J, Garmendia J, et al. SseL, a *Salmonella* deubiquitinase required for macrophage killing and virulence. Proc Natl Acad Sci U S A 2007;104:3502–7.
21. Wilson SM, Bhattacharyya B, Rachel RA, et al. Synaptic defects in ataxia mice result from a mutation in Usp14, encoding a ubiquitin-specific protease. Nat Genet 2002;32:420–5.
22. Meray RK, Lansbury PT, Jr. Reversible monoubiquitination regulates the Parkinson disease-associated ubiquitin hydrolase UCH-L1. J Biol Chem 2007;282:10567–75.
23. Li Z, Melandri F, Berdo I, et al. Δ12-Prostaglandin J2 inhibits the ubiquitin hydrolase UCH-L1 and elicits ubiquitin-protein aggregation without proteasome inhibition. Biochem Biophys Res Commun 2004;319:1171–80.
24. Liu Y, Lashuel HA, Choi S, et al. Discovery of inhibitors that elucidate the role of UCH-L1 activity in the H1299 lung cancer cell line. Chem Biol 2003;10:837–46.
25. Colland F, Formstecher E, Jacq X, et al. Small-molecule inhibitor of USP7/HAUSP ubiquitin protease stabilizes and activates p53 in cells. Mol Cancer Ther 2009;8:2286–95.
26. Bartholomeusz GA, Talpaz M, Kapuria V, et al. Activation of a novel Bcr/Abl destruction pathway by WP1130 induces apoptosis of chronic myelogenous leukemia cells. Blood 2007;109:3470–8.
27. Bartholomeusz G, Talpaz M, Bornmann W, Kong LY, Donato NJ. Degrasyn activates proteasomal-dependent degradation of c-Myc. Cancer Res 2007;67:3912–8.
28. Iwamaru A, Szymanski S, Iwado E, et al. A novel inhibitor of the STAT3 pathway induces apoptosis in malignant glioma cells both *in vitro* and *in vivo*. Oncogene 2007;26:2435–44.
29. Verstovsek S, Manshouri T, Quintas-Cardama A, et al. WP1066, a novel JAK2 inhibitor, suppresses proliferation and induces apoptosis in erythroid human cells carrying the JAK2 V617F mutation. Clin Cancer Res 2008;14:788–96.
30. Foghsgaard L, Wissing D, Mauch D, et al. Cathepsin B acts as a dominant execution protease in tumor cell apoptosis induced by tumor necrosis factor. J Cell Biol 2001;153:999–1010.
31. Dayal S, Sparks A, Jacob J, Allende-Vega N, Lane DP, Saville MK. Suppression of the deubiquitinating enzyme USP5 causes the accumulation of unanchored polyubiquitin and the activation of p53. J Biol Chem 2009;284:5030–41.
32. Borodovsky A, Ovaa H, Kolli N, et al. Chemistry-based functional proteomics reveals novel members of the deubiquitinating enzyme family. Chem Biol 2002;9:1149–59.
33. Borodovsky A, Kessler BM, Casagrande R, Overkleeft HS, Wilkinson KD, Ploegh HL. A novel active site-directed probe specific for deubiquitylating enzymes reveals proteasome association of USP14. EMBO J 2001;20:5187–96.
34. Mullally JE, Fitzpatrick FA. Pharmacophore model for novel inhibitors of ubiquitin isopeptidases that induce p53-independent cell death. Mol Pharmacol 2002;62:351–8.
35. Ding Q, Keller JN. Proteasome inhibition in oxidative stress neurotoxicity: implications for heat shock proteins. J Neurochem 2001;77: 1010–7.
36. Xu P, Duong DM, Seyfried NT, et al. Quantitative proteomics reveals the function of unconventional ubiquitin chains in proteasomal degradation. Cell 2009;137:133–45.
37. Johnston JA, Ward CL, Kopito RR. Aggresomes: a cellular response to misfolded proteins. J Cell Biol 1998;143:1883–98.
38. Kopito RR. Aggresomes, inclusion bodies and protein aggregation. Trends Cell Biol 2000;10:524–30.
39. Kawaguchi Y, Kovacs JJ, McLaurin A, Vance JM, Ito A, Yao TP. The deacetylase HDAC6 regulates aggresome formation and cell viability in response to misfolded protein stress. Cell 2003;115:727–38.
40. Nawrocki ST, Carew JS, Pino MS, et al. Aggresome disruption: a novel strategy to enhance bortezomib-induced apoptosis in pancreatic cancer cells. Cancer Res 2006;66:3773–81.
41. Mullally JE, Moos PJ, Edes K, Fitzpatrick FA. Cyclopentenone prostaglandins of the J series inhibit the ubiquitin isopeptidase activity of the proteasome pathway. J Biol Chem 2001;276:30366–73.
42. Ovaa H, Kessler BM, Rolen U, Galardy PJ, Ploegh HL, Masucci MG. Activity-based ubiquitin-specific protease (USP) profiling of virus-infected and malignant human cells. Proc Natl Acad Sci U S A 2004;101:2253–8.
43. Love KR, Catic A, Schlieker C, Ploegh HL. Mechanisms, biology and inhibitors of deubiquitinating enzymes. Nat Chem Biol 2007;3: 697–705.
44. Yan L, Vatner DE, Kim S-J, et al. Autophagy in chronically ischemic myocardium. Proc Natl Acad Sci U S A 2005;102:13807–12.
45. Amerik A, Swaminathan S, Krantz BA, Wilkinson KD, Hochstrasser M. *In vivo* disassembly of free polyubiquitin chains by yeast Ubp14 modulates rates of protein degradation by the proteasome. EMBO J 1997;16:4826–38.
46. Straus DS, Glass CK. Cyclopentenone prostaglandins: new insights on biological activities and cellular targets. Med Res Rev 2001;21: 185–210.
47. Hershko A, Ciechanover A. The ubiquitin system. Annu Rev Biochem 1998;67:425–79.
48. Daviet L, Colland F. Targeting ubiquitin specific proteases for drug discovery. Biochimie 2008;90:270–83.
49. Hershko A, Rose IA. Ubiquitin-aldehyde: a general inhibitor of ubiquitin-recycling processes. Proc Natl Acad Sci U S A 1987;84:1829–33.
50. Jacobson AD, Zhang N-Y, Xu P, et al. The lysine 48 and lysine 63 ubiquitin conjugates are processed differently by the 26S proteasome. J Biol Chem 2009;284:35485–94.
51. Komander D, Reyes-Turcu F, Licchesi JD, Odenwaelder P, Wilkinson KD, Barford D. Molecular discrimination of structurally equivalent Lys 63-linked and linear polyubiquitin chains. EMBO Rep 2009;10:466–73.
52. Koulich E, Li X, DeMartino GN. Relative structural and functional roles of multiple deubiquitylating proteins associated with mammalian 26S proteasome. Mol Biol Cell 2008;19:1072–82.
53. Johnston SC, Riddle SM, Cohen RE, Hill CP. Structural basis for the specificity of ubiquitin C-terminal hydrolases. EMBO J 1999;18: 3877–87.
54. Hu M, Li P, Li M, et al. Crystal structure of a UBP-family deubiquitinating enzyme in isolation and in complex with ubiquitin aldehyde. Cell 2002;111:1041–54.